BMC Plant Biology

RESEARCH

Open Access

Ameliorating arsenic and PVC microplastic stress in barley (*Hordeum vulgare* L.) using copper oxide nanoparticles: an environmental bioremediation approach

Haifa Abdulaziz Sakit Alhaithloul[1], Suliman Mohammed Suliman Alghanem[2], Ibtisam Mohammed Alsudays[2], Zahid Khorshid Abbas[3], Siham M. AL-Balawi[3], Baber Ali[4,13], Tabarak Malik[5,12*], Sadia Javed[6*], Shafaqat Ali[7,8*], Sezai Ercisli[9,10] and Doaa Bahaa Eldin Darwish[3,11]

Abstract

The present study investigates the impact of varying concentrations of PVC microplastics (PVC–MPs) – specifically 0 (no PVC–MPs), 2, and 4 mg L^{-1} –alongside different arsenic (As) levels of 0 (no As), 150, and 300 mg kg^{-1} in the soil, with the concurrent application of copper oxide–nanoparticles (CuO–NPs) at 0 (no CuO –NPs), 25 and 50 µg mL^{-1} to barley (*Hordeum vulgare* L.) plants. This research primarily aims to assess plant growth and biomass, photosynthetic pigments and gas exchange characteristics, oxidative stress indicators, as well as the response of various antioxidants (both enzymatic and non-enzymatic) and their relevant genes expression, proline metabolism, the AsA–GSH cycle, and cellular fractionation within the plants. The findings showed that increased levels of PVC–MPs and As stress in the soil significantly reduced plant growth and biomass, photosynthetic pigments, and gas exchange characteristics. Additionally, PVC–MPs and As stress increased oxidative stress in the roots and shoots, as evidenced by elevated levels of malondialdehyde (MDA), hydrogen peroxide (H_2O_2), and electrolyte leakage (EL), which in turn stimulated the production of various enzymatic and non-enzymatic antioxidants, gene expression, and sugar content. Furthermore, a notable increase in proline metabolism, the AsA–GSH cycle, and cellular pigmentation was observed. Conversely, the application of CuO–NPs resulted in a substantial improvement in plant growth and biomass, gas exchange characteristics, and the activity of enzymatic and non-enzymatic antioxidants, along with a reduction in oxidative stress. Additionally, CuO–NPs enhanced cellular fractionation while decreasing proline metabolism and the AsA-GSH cycle in *H. vulgare* plants. These outcomes provide new insights into sustainable agricultural practices and offer significant potential in addressing the critical challenges of heavy metal contamination in agricultural soils.

*Correspondence:
Tabarak Malik
tabarak.malik@ju.edu.et
Sadia Javed
sadiajaved@gcuf.edu.pk
Shafaqat Ali
shafaqataligill@yahoo.com

Full list of author information is available at the end of the article

Keywords Cellular component, Gene expression, Heavy metal toxicity, Microplastic, Nanotechnology, Proline metabolism

Introduction

Polyvinyl chloride microplastics (PVC–MPs) represent a pervasive and concerning form of pollution found in various environments, including oceans, rivers, soil, and even the air we breathe [1, 2]. While much attention has been focused on PVC–MPs in aquatic ecosystems, recent studies have also highlighted their presence in soil ecosystems [3, 4]. These PVC–MPs are believed to originate from various sources, contributing to their accumulation and distribution in terrestrial environments. Key sources of soil microplastics include the weathering of larger plastic debris, agricultural activities, the application of wastewater and biosolids, shedding of synthetic fibers, road dust and tire wear, urban runoff, landfill disposal, and the breakdown of plastic products [5, 6]. PVC–MPs can accumulate on the soil surface, creating physical barriers that hinder water regulation and gas exchange [7, 8]. These barriers, in turn, can impede the expansion of plant roots, leading to reduced root growth and overall plant development [1, 9]. Upon exposure to PVC–MPs, plants experience cellular disturbances that trigger increased production of reactive oxygen species (ROS) [10]. This increased ROS activity stimuluses the plant to enhance antioxidant defenses and adjust stress-responsive gene expression to counteract potential oxidative damage [11, 12]. Excessive ROS production can lead to cellular damage and disrupt normal plant metabolism [13, 14]. To effectively address this challenge, a comprehensive understanding of the mechanisms underlying PVC–MPs contamination in soil is necessary. Additionally, strategies need to be developed to mitigate the negative impacts on plants and terrestrial ecosystems. Heavy metals such as arsenic (As) can originate from various sources, including industrial emissions, mining activities, improper waste disposal, and the use of agrochemicals like pesticides and fertilizers [15, 16]. Runoff from urban areas and atmospheric deposition can also contribute to the accumulation of metals in agricultural soil [17]. As a naturally occurring element, As exists in various forms in the environment and is recognized as a significant environmental pollutant due to its toxic effects on both plants and ecosystems [18]. Additionally, As can induce oxidative stress within plant cells by generating ROS [19], which damage cellular structures such as membranes and proteins, potentially leading to cell death [20, 21]. Moreover, As disrupts essential cellular processes by interfering with enzymatic activities and DNA repair mechanisms [19]. Understanding the mechanisms of its toxicity and developing strategies to mitigate its effects are essential for sustainable agriculture and safe food production.

Nanotechnology, which involves the manipulation of materials at the nanoscale level, holds great potential to revolutionize various industries, including agriculture, due to its transformative capabilities [22]. In recent years, novel applications of nanotechnology in agriculture have been explored to enhance crop productivity, improve resource efficiency, and address critical challenges in sustainable food production [23]. Copper oxide nanoparticles (CuO−NPs) have received significant attention due to their distinct physicochemical properties and potential applications, particularly in agriculture [24]. These nanoparticles, characterized by their small size and large surface area to volume ratio, exhibit properties different from their bulk counterparts [25]. In agriculture, CuO−NPs have been investigated for their influence on plant growth, nutrient absorption, and stress responses [26]. Barley (*Hordeum vulgare* L.) is a valuable cereal crop with a rich agricultural heritage. Its versatility and numerous uses have made it a staple in various aspects of human life for centuries [27, 28]. *H. vulgare* plays a crucial role in sustaining global food production as a cereal crop [22]. However, like many other crops, heavy metals and PVC–MPs can negatively impact*H. vulgare*. When the soil is contaminated with elevated levels of heavy metals, barley can absorb and accumulate these elements, leading to hindered plant growth, compromised nutrient absorption, and decreased crop yields [14, 29]. The presence of PVC–MPs in the soil where *H. vulgare* is cultivated can also negatively affect plant growth and development by physically obstructing root growth and limiting the plant's access to water [30]. Therefore, the primary objectives of this study are to identify an effective nanoparticle-based approach to mitigate the toxic impacts of As and PVC–MPs on *H. vulgare* plants. While prior studies have documented the adverse effects of As contamination [17, 31] and MPs [12, 32] on various cereal crops, this study stands out as a novel contribution. Although the combined effects of As and PVC–MPs remain unexplored in this context, particularly under the application of NPs, this study ventures into this previously unexplored area. It examines the combined impact of As and MPs on cereal crop plants, with a distinctive approach that utilizes nanoparticles to counteract these deleterious effects.

Materials and methods

Plant material and cultivation

A pot experiment was conducted in the Biology Department, College of Science, Jouf University, Sakaka 2014, Aljouf, Saudi Arabia, under the glass house. Before sowing, the seeds were carefully washed 10% (v/v) commercial bleach for 10–20 min and then washed with distilled water. Pots were placed under a glass house environment where they received natural sunlight, day/night humidity (60/70%), and day/night temperature (35/40°C), respectively. The physicochemical characteristics of the soil used for the pot study are detailed in Table 1S. Uncontaminated soil from Jouf University, Sakaka 2014, Aljouf, Saudi Arabia research fields was collected. After spiking the soil with As by using sodium arsenate (0, 150, and 300 mg kg^{-1}) in the soil, plastic pots (30-cm-tall * 40-cm-wide) were filled with 10 kg of amended soil and had undergone four different cycles of water equilibration for 2 months and then drying in the air. The same levels of soil were used in a pot experiment previously reported by Saleem et al. [33]. After the addition of sodium arsenate to the soil, PVC–MPs were added as 3.5% w/w of the depth of soil (20 cm) at different concentrations, i.e., 0, 2, and 4 mg L^{-1} PVC–MPs as discussed in the review of literature by Ge at al. [34]. A moisture level of 70% was maintained throughout the experiment by irrigating the plants with deionized water free of As and PVC–MPs. The total duration of experimental treatments was two months under controlled conditions. Experiment was conducted in completely randomized design (CRD) with four replications of each treatment and one plant was used in each pot. All chemicals used in the experiment were of analytical grade and provided by Sinopharm Chemical Reagent Co., Ltd. Refer to Fig. 1 for a detailed layout of the experimental setup involving *H. vulgare* plants in a controlled glasshouse environment.

Experimental treatments

In this pot experiment, we have used three different levels of PVC−MPs and As stress along with the control which were foliar supplied with three different levels of CuO−NPs. As We have displayed the PVC−MPs and As treatments separately, hence, the treatment design

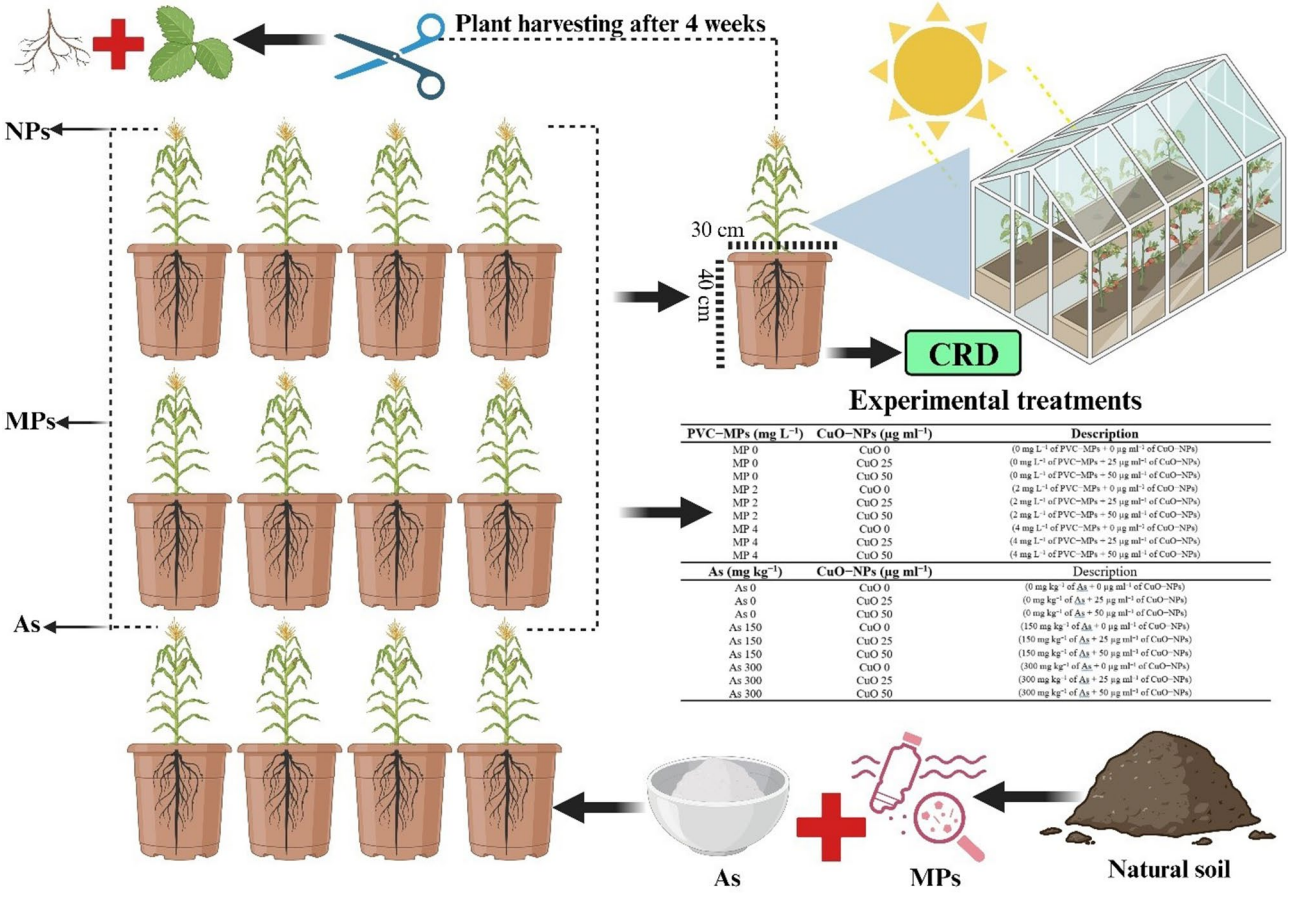

Fig. 1 Schematic layout of *H. vulgare* plants sown in the pots and placed in a controlled glasshouse environment. The experiment was conducted in a CRD with four replications and harvested after four weeks of seed sowing. Artificial addition of As and PVC−MPs was supplied artificially, and plants were also treated with CuO−NPs

for PVC−MPs and As stress with the application of CuO−NPs are as follow in the Table 4S.

Synthesis and characterization of *CuO−NPs*

CuO−NPs powder was purchased from US Research Nanomaterials, Inc (Houston, TX). The size and shape of CuO−NPs are spherical. The size of CuO−NPs ranged from 9 to 22 nm in diameter, with an average diameter of 14.3 nm, as determined by measuring over 25 and 50 µg ml^{-1} CuO−NPs with Image J (ver 1.51). The hydrodynamic size and zeta potential of CuO−NPs at 25 and 50 µg ml^{-1} in tap water after one hour of mixing was determined with a Malvin Zetasizer Nano ZS (Westborough, MA). The hydrodynamic size of CuO−NPs was 593.9±22.8 nm, indicating significant aggregation. The NPs possessed a negative surface charge and the measured zeta potential was −39.0±1.4 nm [26]. The CuO−NPs exhibited a purity level of 97% and had particle sizes ranging from 0 to 50 nm.

Sampling and data collection

After two months, the remaining three seedlings were carefully uprooted and gently washed with distilled water to remove any airborne dust and surface deposition. Functional leaf in each treatment was picked at a rapid growth stage during 09:00–10:30. The sampled leaves were washed with distilled water, immediately placed in liquid nitrogen, and stored in a freezer at −80 °C for further analysis. All of the harvested plants were divided into two parts (i.e., roots and shoots) to study different physio-biochemical traits. Leaves from each treatment group were picked for chlorophyll, carotenoid, oxidative stress, and antioxidants analysis. Root and shoot lengths were measured straightway after the harvesting by using measuring scale and digital weighting balance to measure fresh biomass. Number of leaves were measured by simple counting the leaves while leaf area was also measured. Roots were uprooted and immersed in 20-mM ethylenediaminetetraacetic acid disodium salt (Na_2EDTA) for 15–20 min to remove As adhered to the root surfaces. Then, roots were washed thrice with distilled water and, finally, once with de-ionized water, and dried for further analysis. The different parts of the plant (i.e., roots and shoots) were oven-dehydrated at 65 °C for 72 h for As determination, and the total plant dry weight was also measured. Although this experiment was conducted in pots, for the collection of organic acids, two seedlings were transferred to the rhizoboxes which consist of plastic sheet, nylon net, and wet soil [35]. After 48 h, plants were taken from the rhizoboxes and the roots were washed with redistilled water to collect the exudates from root surface. The samples were filtered through a 0.45- µm flter (MillexHA, Millipore) and collected in eppendorf tubes [36]. The collected samples were mixed with NaOH (0.01 M) in order to analyze the organic acids. However, the samples used for analysis of oxalic acid were not treated with NaOH [35].

Determination of chlorophyll pigments and gas exchange parameters

Leaves were collected for the determination of chlorophyll and carotenoid contents. For chlorophylls, 0.1 g of fresh leaf sample was extracted with 8 mL of 95% acetone for 24 h at 4 °C in the dark. The absorbance was measured by a spectrophotometer (UV-2550; Shimadzu, Kyoto, Japan) at 646.6, 663.6, and 450 nm. Chlorophyll content was calculated by the standard method of [37].

Net photosynthesis (P*n*), leaf stomatal conductance (G*s*), transpiration rate (T*s*), and intercellular carbon dioxide concentration (C*i*) were measured from four different plants in each treatment group. Measurements were conducted between 11:30 and 13:30 on days with a clear sky. Rates of leaf P*n*, G*s*, T*s*, and C*i* were measured with a LI-COR gas-exchange system (LI-6400; LI-COR Biosciences, Lincoln, NE, USA) with a red-blue LED light source on the leaf chamber. In the LI-COR cuvette, CO_2 concentration was set as 380 mmol mol^{-1} and LED light intensity was set at 1000 mmol m^{-2} s^{-1}, which was the average saturation intensity for photosynthesis in *H. vulgare* [38].

Determination of oxidative stress indicators

The degree of lipid peroxidation was evaluated as malondialdehyde (MDA) contents. Briefly, 0.1 g of frozen leaves were ground at 4 °C in a mortar with 25 mL of 50 mM phosphate buffer solution (pH 7.8) containing 1% polyethene pyrrole. The homogenate was centrifuged at 10,000 × *g* at 4 °C for 15 min. The mixtures were heated at 100 °C for 15–30 min and then quickly cooled in an ice bath. The absorbance of the supernatant was recorded by using a spectrophotometer (xMark™ Microplate Absorbance Spectrophotometer; Bio-Rad, United States) at wavelengths of 532, 600, and 450 nm. Lipid peroxidation was expressed as l mol g^{-1} by using the formula: 6.45 (A532-A600)-0.56 A450. Lipid peroxidation was measured by using a method previously published by Health and Packer [39].

To estimate H_2O_2 content of plant tissues (root and leaf), 3 mL of sample extract was mixed with 1 mL of 0.1% titanium sulfate in 20% (v/v) H_2SO_4 and centrifuged at 6000×g for 15 min. The yellow colour intensity was evaluated at 410 nm. The H_2O_2 level was computed by the extinction coefficient of 0.28^{-1} cm^{-1}. The contents of H_2O_2 were measured by the method presented by Jana and Chaudhary [40].

Stress-induced electrolyte leakage (EL) of the uppermost stretched leaves was determined by using the methodology of Dionisio-Sese and Tobita [41]. The leaves

were cut into minor slices (5 mm length) and placed in test tubes having 8 mL distilled water. These tubes were incubated and transferred into a water bath for 2 h prior to measuring the initial electrical conductivity (EC_1). The samples were autoclaved at 121 °C for 20 min and then cooled down to 25 °C before measuring the final electrical conductivity (EC_2). Electrolyte leakage was calculated by the following formula;

$$EL = (EC_1/EC_2) \times 100$$

Determination of antioxidant enzyme activities and relative gene expression

To evaluate enzyme activities, fresh leaves (0.5 g) were homogenized in liquid nitrogen and 5 mL of 50 mmol sodium phosphate buffer (pH 7.0), including 0.5 mmol EDTA and 0.15 mol NaCl. The homogenate was centrifuged at 12,000 × *g* for 10 min at 4 °C, and the supernatant was used for measurement of superoxidase dismutase (SOD) and peroxidase (POD) activities. SOD activity was assayed in 3 mL reaction mixture containing 50 mM sodium phosphate buffer (pH 7), 56 mM nitro blue tetrazolium, 1.17 mM riboflavin, 10 mM methionine, and 100 µL enzyme extract. Finally, the sample was measured by using a spectrophotometer (xMark™ Microplate Absorbance Spectrophotometer; Bio-Rad). Enzyme activity was measured by using a method by Chen and Pan [42] and expressed as U g^{-1} FW.

Peroxidase activity in the leaves was estimated by using the method of Sakharov and Ardila [43] by using guaiacol as the substrate. A reaction mixture (3 mL) containing 0.05 mL of enzyme extract, 2.75 mL of 50 mM phosphate buffer (pH 7.0), 0.1 mL of 1% H_2O_2, and 0.1 mL of 4% guaiacol solution was prepared. Increases in the absorbance at 470 nm because of guaiacol oxidation was recorded for 2 min. One unit of enzyme activity was defined as the amount of the enzyme.

Catalase (CAT) activity was analyzed according to Aebi [44]. The assay mixture (3.0 mL) was comprised of 100 µL enzyme extract, 100 µL H_2O_2 (300 mM), and 2.8 mL 50 mM phosphate buffer with 2 mM ETDA (pH 7.0). The CAT activity was measured from the decline in absorbance at 240 nm as a result of H_2O_2 loss (ε=39.4 mM^{-1} cm^{-1}).

Ascorbate peroxidase (APX) activity was measured according to Nakano and Asada [45]. The mixture containing 100 µL enzyme extract, 100 µL ascorbate (7.5 mM), 100 µL H_2O_2 (300 mM), and 2.7 mL 25 mM potassium phosphate buffer with 2 mM EDTA (pH 7.0) was used for measuring APX activity. The oxidation pattern of ascorbate was estimated from the variations in wavelength at 290 nm (ε=2.8 mM^{-1} cm^{-1}).

Quantitative real-time PCR (RT-qPCR) assay was applied to investigate the expression levels of 4 stress-related genes, including Fe-SOD, POD, CAT and APX. Total RNA was extracted from leaf tissue samples using RNeasy Plant Mini kits (Qiagen, Manchester, UK). Contaminating DNA was then removed and first-strand cDNAs were prepared using Reverse Transcription kits (Qiagen, Manchester, UK). RT-qPCR analysis was conducted as reported in the protocol of QuantiTect SYBR Green PCR kit (Qiagen, Manchester, UK). Reaction volume and PCR amplification conditions were adjusted as mentioned by El-Esawi [46]. The gene amplifications of Sirhindi et al. [47] of the following genes are given in Table 2S.

Determination of osmolytes and sugars

Plant ethanol extracts were prepared for the determination of non-enzymatic antioxidants and some key osmolytes. For this purpose, 50 mg of dry plant material was homogenized with 10 mL ethanol (80%) and filtered through Whatman No. 41 filter paper. The residue was re-extracted with ethanol, and the 2 extracts were pooled together to a final volume of 20 mL. The determination of flavonoids [48], phenolics [49], anthocyanin [50], and total sugars [51] was performed from the extracts.

Determination of proline related attributes

To measure proline concentrations, 0.5 g of shoot tissues were ground in sulfosalicylic acid and then centrifuged, and the supernatant was collected from each sample. The proline concentration in each sample was measured [52]. Specifically, the supernatant from each sample was reacted with acid ninhydrin, and the resulting colorimetric reaction was measured to determine the proline concentration by "UV-1700 pharmaSpec spectrophotometer".

The ProDH "proline dehydrogenase", P5CR "pyrroline-5-carboxylate reductase", and P5C "pyrroline-5-carboxylate" were measured using kits provided by Jiangsu Meibiao Biological Technology Co., Ltd. Enzyme activities were accurately measured using these reagent kits, which include all chemicals and related instructions by "UV-1700 pharmaSpec spectrophotometer".

Determination of AsA-GSH cycle

Glutathione (GSH), glutathione disulfide (GSSH), DHA (dehydroascorbic acid), and ascorbic acid (AsA) were determined in fresh leaves [53] and were extracted by homogenizing 0.2 g of leaves in TCA and then collecting the supernatant by centrifugation. GSH concentration was measured in a solution including phosphate buffer, supernatant, and DTNB reagent (PBS, pH 7.0) [53]. The amount of GSH was determined by a spectrophotometer. To measure the AsA content, NaH_2PO_4 solution, enzyme

extract, distilled water, and 10% TCA were mixed to determine the concentration of AsA in the samples [53]. After a 30-s incubation period, $FeCl_3$ solution, H_3PO_4, and 2,2′ -dipyridine were added to the reaction mixture. The $FeCl_3$ and 2,2′ -dipyridine reacted with the AsA to produce a red-colored complex that can be measured spectrophotometrically at 525 nm. The amount of AsA present in the sample was calculated.

Determination of cell wall component fractionation

Cell wall isolation was done as reported by Yang et al. [54]. Shoots (4 g) were placed in a mortar and ground with liquid nitrogen. The homogenized samples were transferred to centrifuge tubes and 75% ethanol was added and incubated at 25 °C. The samples were centrifuged. The bottom sediment was further homogenized in 10 mL of each of acetone, chloroform, and methanol (v: v=1:1) for 30 min each, with shaking at room temperature. The homogenate was centrifuged. The remaining cell wall components were lyophilized until dry sediment was obtained. The lyophilized cell wall components were analyzed for biochemical assays. Subsequently, the separation of the hemicellulose fraction was carried out [54]. Approximately 3 mg CW was mixed with water in an Eppendorf tube. The mixture was boiled for 1 h using a heating block or hot plate set at 100 ∘C and centrifuged. The above procedure was repeated for duplicate samples. After 12 h, the precipitate was extracted twice with 1 mL of KOH (24%, w/v) at room temperature. After each extraction, centrifugation was done. The hemicellulose concentration was measured at 540 nm absorbance.

Pectin Assay Kit was used to detect pectin. Pectinesterase Assay Kit was used to detect PME activity. The Cellulose Assay Kit was used to detect cellulose concentrations using kits provided by Jiangsu Meibiao Biological Technology Co., Ltd. Enzyme activities were accurately measured using these reagent kits, which include all chemicals and related instructions. DM was calculated using the formula: demethylation degree=100 - DM, where DM is the degree of methylation.

As uptake and accumulation factors

For the determination of total As concentration in shoots and roots, samples were oven-dried at 65 °C for 24 h and ashed in a muffle furnace at 550 °C for 20 h. After that, the ash was incubated with 31% (m/v) HNO_3 and 17.5% (v/v) H_2O_2 at 70 °C for about 2 h and added distilled water. The As concentration in the digest was determined using an atomic absorption spectrophotometer (AAS).

Bioaccumulation factor (BAF) was calculated as the ratio of As concentration in tissues and As concentration in nutrient medium by using the following formula:

$$\text{BAF} = \text{As concentration (plant tissues)} \,/\, \text{As concentration (Soil)}$$

while translocation factor (TF) was determined by estimating the concentration of As in one part of plant with respect to the other parts as follow:

$$\text{TF} = \text{As concentration (shoots)} \,/\, \text{As concentration } (roots)$$

Statistical analysis

The normality of data was analyzed using IBM SPSS software (Version 21.0. Armonk, NY, USA: IBM Corp) through a multivariate post-hoc test, followed by Duncan's test to determine the interaction among significant values. Thus, the differences between treatments were determined by using ANOVA, and the least significant difference test ($P<0.05$) was used for multiple comparisons between treatment mean values where significant. Tukey's HSD post-hoc test was used to compare the multiple comparisons of mean values. The analysis showed that the data in this study were almost normally distributed. The graphical presentation was carried out using Origin-Pro 2017. The plots of principal component, heatmap and correlation analysis on *H. vulgare* parameters were carried out using the RStudio software.

Results

Plant growth and photosynthetic apparatus

In the present study, various growth parameters and photosynthetic pigments and also the gas exchange parameters in *H. vulgare* under the PVC-MPs and As stress with the application of CuO-NPs were measured. Growth and biomasses of *H. vulgare* are presented in Fig. 2, while gas exchange attributes are presented in Fig. 1S. Specifically, we observed significant ($P<0.05$) decrease in root length, shoot length, leaf count, leaf area, shoot fresh weight, root fresh weight, shoot dry weight, root dry weight, as well as reductions in chlorophyll a, chlorophyll b, chlorophyll a/b ratio, carotenoid content, net photosynthesis, stomatal conductance, transpiration rate and intercellular CO_2 (Figs. 1S and 2). However, application of CuO-NPs caused increase in root length, shoot length, leaf count, leaf area, shoot fresh weight, root fresh weight, shoot dry weight, root dry weight, as well as reductions in chlorophyll a, chlorophyll b, chlorophyll a/b ratio, carotenoid content, net photosynthesis, stomatal conductance, transpiration rate and intercellular CO_2 compared to the plants which were grown without the application of CuO-NPs.

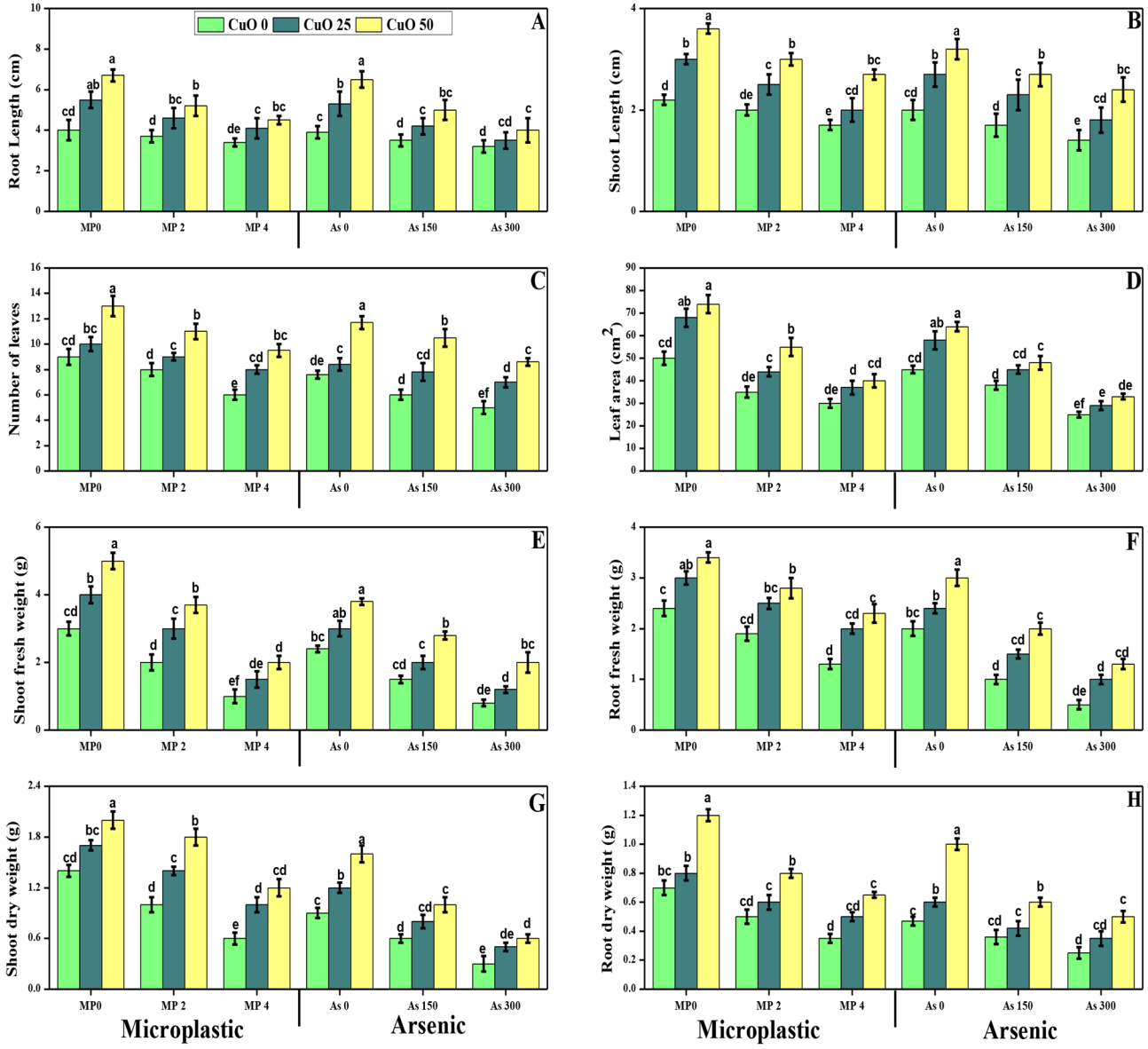

Fig. 2 Impact of microplastics [0 (no microplastic), 2 and 4 mg L^{-1} PVC – microplastic] and arsenic [0 (no As), 150, and 300 mg kg^{-1}] on morphological traits i.e., root length (**A**), shoot length (**B**), leaf count (**C**), leaf area (**D**), shoot fresh weight (**E**), root fresh weight (**F**), shoot dry weight (**G**) and root dry weight (**H**) is depicted under the application of CuO-NPs i.e., 0, 25 and 50 µg ml^{-1} in *H. vulgare* (barley). Duncan's multiple range test ($P < 0.05$) reveals (using two-way ANOVA) significant differences among bars indicated by different letters for each parameter

Oxidative stress and response of antioxidant capacity

In the present study different oxidative stress biomarkers i.e., malondialdehyde (MDA), hydrogen peroxide (H_2O_2) and electrolyte leakage (EL) were measured from the roots and leaves of *H. vulgare* as presented in (Fig. 2S). According to the results, it was observed that the PVC-MPs and As stresses caused a significant increase in MDA, EL and H_2O_2 content in the roots and leaves of the plants compared to the plants which were not grown in the toxic levels of PVC-MPs and As stress in the soil. Although the application of CuO-NPs decreases the MDA, EL and H_2O_2 content in the roots and leaves of *H. vulgare* under the all studied levels of PVC-MPs and As toxicity in the soil.

Different enzymatic antioxidants i.e., superoxidase dismutase (SOD), ascorbate peroxidase (APX), peroxidase (POD), catalase (CAT) and non-enzymatic compounds i.e., phenolic, anthocyanin, flavonoids, ascorbic acid and flavonoid and also their relevant gene expression i.e., SOD, POD, CAT and APX were also measured from the roots and leaves of *H. vulgare*. The results regarding the enzymatic antioxidants and their specific gene expressions are presented in Fig. 3S, and the results regarding the non-enzymatic compounds are presented in

Fig. 4S. According to the results, we have noticed that the PVC-MPs and As toxicity in the soil significantly increases the enzymatic antioxidants i.e., SOD, POD, CAT and APX and their relevant gene expression and also the non-enzymatic compounds i.e., phenolic, anthocyanin, flavonoids, ascorbic acid and flavonoid compared to the plants grown without the toxic concentration of PVC-MPs and As toxicity in the soil. Present findings also showed that the application of CuO-NPs also increases the activity of SOD, POD, CAT and APX and their relevant gene expression and also the non-enzymatic compounds i.e., phenolic, anthocyanin, flavonoids, ascorbic acid and flavonoid compared to the plants which were not treatment with the application of CuO-NPs. In addition, the maximum activity of SOD, POD, CAT and APX and their relevant gene expression and also the non-enzymatic compounds i.e., phenolic, anthocyanin, flavonoids, ascorbic acid and flavonoid were observed in the plants which grown in the application of CuO-NPs under the toxic levels of PVC-MPs and As concentration in the soil.

Sugars, proline related parameters, AsA-GSH cycle and cellular fractionation

In the present study, total sugar and reducing sugar were also measured from the *H. vulgare* under the PVC-MPs and As stress and presented in Fig. 4S(E-F). The proline related attributes are presented in Fig. 5S and AsA-GSH cycle is presented in Fig. 6S. According to the given results, it was noticed that the PVC-MPs and As toxicity in the soil significantly decreased the total sugar and reducing sugar compared to the control. However, the application of CuO-NPs caused a significant increase in the total sugar and reducing sugar compared to those plants which were grown in without the application of CuO-NPs.

The proline related parameters such as proline, pyrroline-5-carboxylate, pyrroline-5-carboxylate reductase and pyrroline-5-carboxylate dehydrogenase were also measured from the *H. vulgare* tissue and results showed that the PVC-MPs and As toxicity induced a significant decrease in the proline, pyrroline-5-carboxylate and pyrroline-5-carboxylate reductase compared to the control except the pyrroline-5-carboxylate dehydrogenase (Fig. 5S). However, the application of CuO-NPs induced a significant decrease in the content of proline, pyrroline-5-carboxylate, pyrroline-5-carboxylate reductase, compared to those plants which were grown without the application of CuO-NPs except the pyrroline-5-carboxylate dehydrogenase.

AsA-GSH cycle including the contents of glutathione, ascorbate, glutathione disulfide, dehydroascorbic acid were also measured and we have noticed that the PVC-MPs and As toxicity significantly decreases the content of glutathione, ascorbate and dehydroascorbic acid while increases the content of glutathione disulfide from the tissues of the *H. vulgare* (Fig. 6S). However, the application of CuO-NPs increases the contents of glutathione, ascorbate and dehydroascorbic acid compared to the plants which were grown without the application of CuO-NPs. Cellular compartments fractionation i.e., pectin methylesterase activity, uronic acid, hemicellulose I, hemicellulose II, cellulose and pectin methylesterase were also determined from the *H. vulgare* and presented as Fig. 7S. Results from the present study showed that the PVC-MPs and As toxicity causes a significant increase in the pectin methylesterase activity, uronic acid, hemicellulose I, hemicellulose II, cellulose and pectin methylesterase when compared to the control. However, application of CuO-NPs further increases the content of pectin methylesterase activity, uronic acid, hemicellulose I, hemicellulose II, cellulose and pectin methylesterase in *H. vulgare*.

Bioaccumulation factor and translocation factor

In our study, As content from the different parts of plants were measured in As stressed and also PVC−MPs stressed *H. vulgare* plants as presented in Table 3S. A rare concentration of As was observed in the plants when cultivated in PVC−MPs stressed with or without the application of CuO-NPs. However, we have noticed that the increasing levels of As in the soil induced a significant increase in As content in various parts of *H. vulgare*, while maximum increased was observe in the plants which were grown in the 300 mg kg^{-1} of As. We have also noticed that the application of CuO-NPs significantly decreased the concentration of As in all parts of the plants and these results were observed under all levels of As in the soil i.e., 150 and 300 mg kg^{-1} of As.

Bioaccumulation factor (BAF) (Fig. 3A) and TF (Fig. 3B) was also calculated from the *H. vulgare* under the NPs application. All the values of BAF were less than 1 while maximum BAF was noticed in roots of *H. vulgare* which increases due to increase in As stress while the BAF decreases when the *H. vulgare* were applied with various levels of CuO-NPs application. Similarly, translocation factor (TF) was decreases due to the application of CuO-NPs at all levels of As stress. In addition, all the values of TF are less than 1 which were increases due to elevate level of As in the soil.

Correlation between as uptake and different growth and photosynthetic parameters in *H. vulgare*

A Pearson's correlation graph was constructed to quantify the relationship between various growth parameters with As uptake in different parts of the plant (Fig. 4). As concentration in the roots was positively correlated with As concentration in the leaves, tillers and stems, but

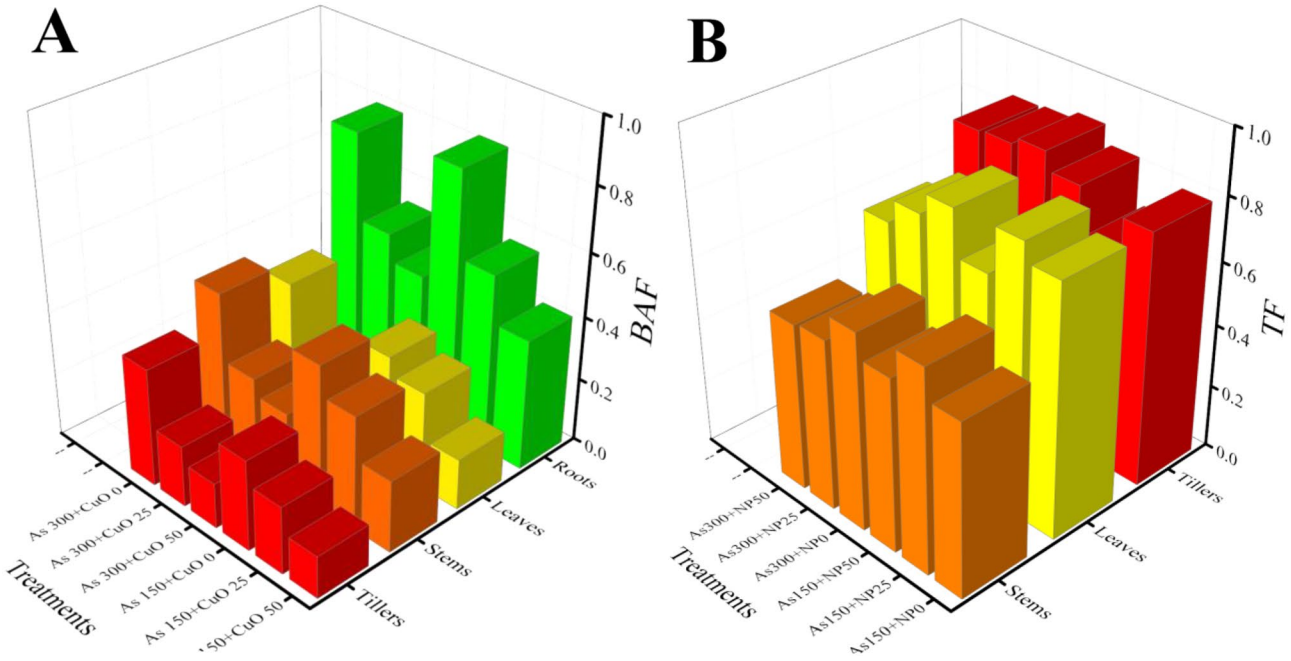

Fig. 3 (**A**) Bioaccumulation factor (BAF) and (**B**) translocation factor (TF) values for As in *H. vulgare* plants influenced by CuO-NPs application

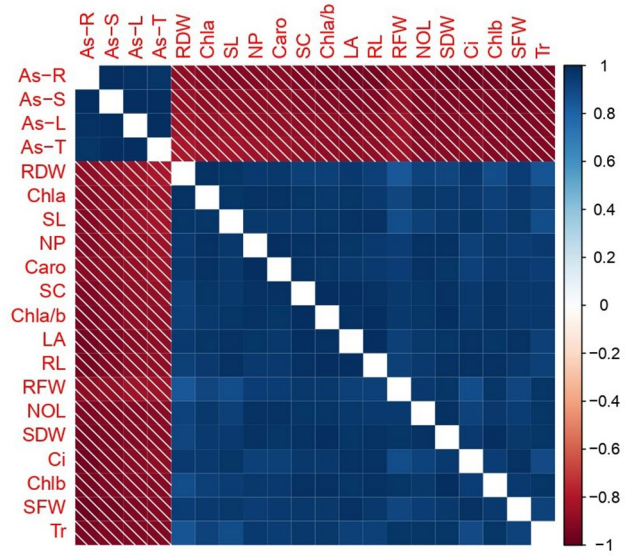

Fig. 4 Correlation between As uptake and growth-photosynthetic parameters in *H. vulgare* plants. The diagram demonstrates a direct correlation between As uptake in the roots and shoots. Conversely, there's an inverse relationship between As uptake and the growth and photosynthetic efficiency of *H. vulgare* plants. Different parameters along with their abbreviations used in this figure are as follow: As-R (arsenic concentration in the roots), As-S (arsenic concentration in the stem), As-L (arsenic concentration in the leaves), As-T (arsenic concentration in the tillers), RDW (root dry weight), Chla (chlorophyll-a content), SL (shoot length), NP (net photosynthesis), Caro (carotenoid content), SC (stomatal conductance), Chla/b (chlorophyll a/b content), LA (leaf area), RL (root length), RFW (root fresh weight), NOL (number of leaves), SDW (shoot dry weight), Ci (intercellular CO_2), Chlb (chlorophyll-b content), SFW (shoot fresh weight) and Tr (transpiration rate)

negatively correlated with root dry weight, chlorophyll-a content, shoot length, net photosynthesis, carotenoid content, stomatal conductance, chlorophyll a/b content, leaf area, root length, root fresh weight, number of leaves, shoot dry weight, intercellular CO_2, chlorophyll-b content, shoot fresh weight and transpiration rate. Similarly, As concentration in the stems was positively correlated with As concentration in the leaves, tillers and toots, but negatively correlated with root dry weight, chlorophyll-a content, shoot length, net photosynthesis, carotenoid content, stomatal conductance, chlorophyll a/b content, leaf area, root length, root fresh weight, number of leaves, shoot dry weight, intercellular CO_2, chlorophyll-b content, shoot fresh weight and transpiration rate. This correlation is depicted a close connection between As uptake and growth in *H. vulgare*.

Principal component analysis

The loading plots of principal component analysis (PCA) to evaluate the effect of different levels of As in the soil with the application of CuO−NPs on different attributes of *H. vulgare* are presented in Fig. 5. Of all the main components, the first two components—Dim1 and Dim2—comprise more than 97% of the whole database and make up the largest portion of all components (Fig. 5). Among this, Dim1 contributes 94.2%, and Dim2 contributes 3.1% of the whole dataset. In addition, Fig. 5 also shows that As contents in roots and leaves, tillers and stems, were positively correlated in the dataset from all the variables. In contrast, root dry weight, chlorophyll-a content, shoot length, net photosynthesis, carotenoid content, stomatal

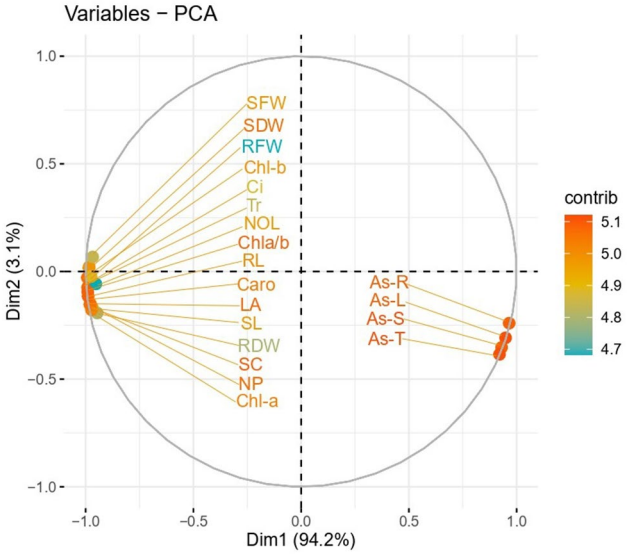

Fig. 5 Loading plots of principal component analysis (PCA) on different studied attributes of *H. vulgare* grown under various stress levels of As and PVC−MPs in the soil under the application of CuO−NPs. Different parameters along with their abbreviations used in this figure are as follow: As-R (arsenic concentration in the roots), As-S (arsenic concentration in the stem), As-L (arsenic concentration in the leaves), As-T (arsenic concentration in the tillers), RDW (root dry weight), Chla (chlorophyll-a content), SL (shoot length), NP (net photosynthesis), Caro (carotenoid content), SC (stomatal conductance), Chla/b (chlorophyll a/b content), LA (leaf area), RL (root length), RFW (root fresh weight), NOL (number of leaves), SDW (shoot dry weight), Ci (intercellular CO_2), Chlb (chlorophyll-b content), SFW (shoot fresh weight) and Tr (transpiration rate)

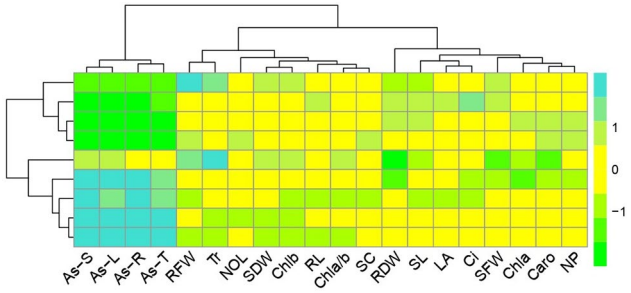

Fig. 6 Heat-map analysis highlighting relationships between various *H. vulgare* parameters including plant growth and biomass, photosynthetic pigments, gas exchange characteristics and As accumulation from different parts of the plants, under the application of CuO−NPs. Different parameters along with their abbreviations used in this figure are as follow: As-R (arsenic concentration in the roots), As-S (arsenic concentration in the stem), As-L (arsenic concentration in the leaves), As-T (arsenic concentration in the tillers), RDW (root dry weight), Chla (chlorophyll-a content), SL (shoot length), NP (net photosynthesis), Caro (carotenoid content), SC (stomatal conductance), Chla/b (chlorophyll a/b content), LA (leaf area), RL (root length), RFW (root fresh weight), NOL (number of leaves), SDW (shoot dry weight), Ci (intercellular CO_2), Chlb (chlorophyll-b content), SFW (shoot fresh weight) and Tr (transpiration rate)

conductance, chlorophyll a/b content, leaf area, root length, root fresh weight, number of leaves, shoot dry weight, intercellular CO_2, chlorophyll-b content, shoot fresh weight and transpiration rate were negatively correlated in the dataset from all the variables (Fig. 5).

Heatmap analysis

In our study, we have also exhibited a heat-map analysis to gain insights into the different parameters of *H. vulgare*, including plant growth and biomass, photosynthetic pigments, gas exchange characteristics and As accumulation from different parts of the plants under the application of CuO−NPs (refer to Fig. 6). Results from the present study showed that most of the studied parameters showed non-significant relationship when the *H. vulgare* was subjected to PVC−MPs and As stress, even with the application of CuO−NPs. Although, As accumulation from different parts of the plants showed a non-significant relation compare to other studied parameters.

Discussion

Negative impact of PVC−MPs on crop growth and ecophysiology

Plants grown in agricultural soils are directly exposed to MPs when plastic mulching, sewage sludge as fertilizer, and organic manures are applied [3, 4]. PVC−MPs particles of bigger size (100 nm–5 mm) can be indirectly harmful to plants through modifying and/or disrupting the soil structure. But it can also affect directly through clogging the seed pores [7, 8]. Several studies have reported the effects of MPs on terrestrial plants grown in soil, showed a negative impact on plant growth and biomass [30, 55]. Although, the toxic effects of MPs depend upon the plastic type, particle size, and exposure dose. PVC−MPs−mediated alterations in plant cellular functions lead to an imbalance in redox reactions, favoring the overproduction of ROS. This surge in ROS, driven by PVC−MPs interference, disrupts cellular homeostasis and precipitates oxidative damage in plant tissues and also induces cellular fractionation and disturbs AsA−GSH cycle [56]. Elevated concentrations of PVC−MPs induce oxidative stress (Fig. 2S) and subsequently lead to a reduction in plant growth (Fig. 1) and photosynthetic efficiency (Fig. 1S). When PVC−MPs are present in the soil, they can release toxic additives, absorb pollutants, and create physical barriers that affect plant−root interactions [11, 12]. In addition, PVC−MPs in the soil can disrupt root architecture and function, impairing water uptake and leading to inhibited plant growth and photosynthetic machinery, as shown in *Ipomoea batatas* [9] and *Oryza sativa* [57].

In addition, ROS accumulation can damage cellular components, including lipids, proteins, and DNA, impairing cellular function and overall plant

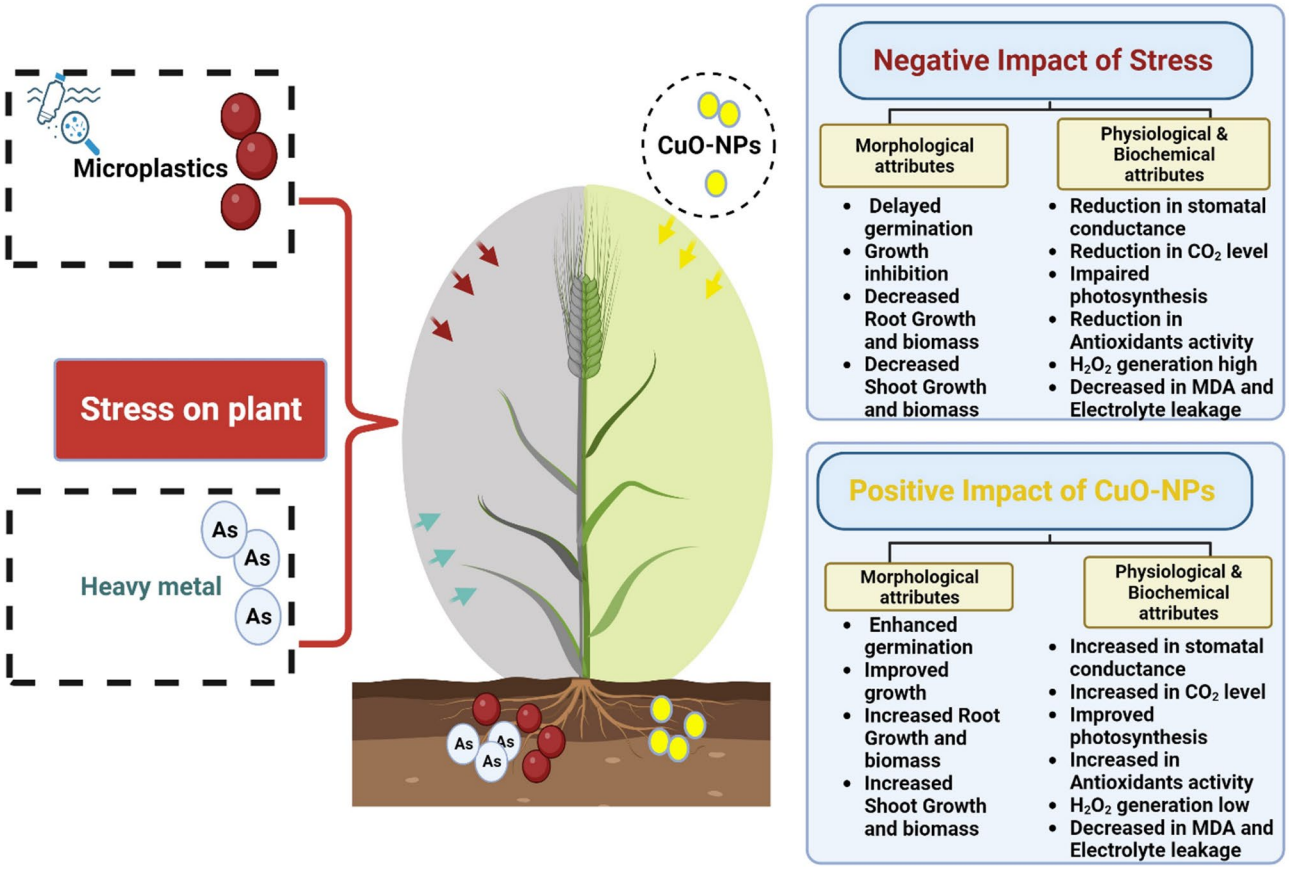

Fig. 7 Comprehensive overview of the effects of PVC – MPs and As toxicity on *H. vulgare* plants and the mitigative role of CuO – NPs. The combined stress from PVC – MPs and As reduces growth and impairs the photosynthetic machinery in *H. vulgare*, leading to an increase in ROS and subsequent oxidative stress. This stress also disrupts the AsA-GSH cycle, alters proline-related contents, and triggers cellular fractionation. Notably, the application of CuO – NPs effectively alleviates these adverse impacts by increasing antioxidant machinery and captured extra ROS; thus, ultimately improved plant growth

development [58]. Proline biosynthesis primarily involves two enzymatic steps: the conversion of glutamate to pyrroline-5-carboxylate (P5C) catalyzed by Δ1-pyrroline-5-carboxylate synthase (P5CS), and the subsequent reduction of P5C to proline via pyrroline-5-carboxylate reductase (P5CR), as shown in *Lepidium sativum* by [59]. Plant GSH levels are affected by PVC – MPs toxicity, which may lead to oxidative damage. Proline and its related parameters act as an osmolyte, stabilizing cellular structures and enzymes under stress conditions, thereby assisting plants in mitigating the adverse effects of PVC – MPs-induced stress. The AsA-GSH (ascorbate-glutathione) cycle is a vital antioxidant defense mechanism in plants which detoxifies H_2O_2 and maintains a balance of reduced and oxidized forms of ascorbate and glutathione, thereby preserving cellular redox homeostasis and protecting the cell from oxidative damage [60, 61]. This cycle involves the interplay of two major antioxidant molecules: ascorbate (AsA, also known as vitamin C) and glutathione (GSH). This mechanism not only detoxifies ROS but also helps protect cellular components from oxidative damage, contributing to the overall resilience of plants under PVC – MPs toxicity [16]. The plant cell wall is a complex and dynamic structure composed of various components, including cellulose, hemicellulose, pectin, lignin, and proteins. These components collectively provide structural integrity, mechanical support, and protection to plant cells and are affected by PVC – MPs toxicity.

Negative impact of as on crop growth and ecophysiology

As toxicity has become a prevalent issue in agricultural as it interferes with the chloroplast's structure and function, leading to reduced chlorophyll synthesis, diminished light absorption, hindered electron transport, and decreased carbon assimilation [18]. As – induced alterations in chloroplast morphology impair photosynthetic processes, resulting in decreased light-harvesting capabilities and inefficient carbon fixation [19]. Numerous reports indicate that escalating levels of As in the soil have resulted in adverse effects on plants, manifesting as negative impacts on their growth and overall yield [15, 62]. As uptake disrupts cellular redox equilibrium, leading to an overproduction of ROS. This imbalance overwhelms the plant's antioxidant enzymatic defenses,

rendering them ineffective in countering ROS-induced oxidative damage [19]. In response to As stress, plant cells activate specific signaling pathways that trigger the transcriptional machinery to upregulate genes essential for detoxification, stress tolerance, and repair mechanism [63]. As stress induces the production of secondary metabolites, such as phenolics, flavonoids, anthocyanin, and ascorbic acid, which aid in metal detoxification and protection against oxidative damage [64]. Through As stress, the accumulation of oxidized forms of glutathione and ascorbic acid, which are markers of oxidative damage, can be reduced, increasing the antioxidant capacity of the plant [21]. The mechanism governing proline production under metal stress is multifaceted, reflecting the plant's adaptive response to mitigate the impact of heavy metal toxicity [17]. Cell wall in plants is responsible for the development of stress tolerance to metals and nonmetals. In addition, cell wall can form a hard structure that prevents toxic ions from entering the cytoplasm [18]. Polysaccharides found in cell wall include cellulose, hemicellulose, and pectin, all of which can change in response to environmental stress [33]. For example, pectin methyl esterase can change the level of pectin methylation and thus the number of As ions bound to the cell wall [31]. The influence of metal stress on cellular components within plants is governed by intricate mechanisms involving multiple physiological and biochemical processes, such as secondary metabolite production, cell division and growth, enzyme inhibition and cell membrane integrity [65].

Ameliorative impact of CuO-NPs on crop growth and ecophysiology

Nanotechnology has gained immense popularity in recent times and has emerged as a prominent and widely discussed subject across various scientific disciplines. Its application spans a multitude of fields, heralding transformative advancements and innovations [22]. The mechanism through which NPs counteract abiotic stress involves intricate interactions at the molecular and physiological levels, including ROS scavenging, enhanced nutrient uptake, improved photosynthesis, gene expression modulation, biological nano-fertilization [23]. NPs possess the ability to bind and deliver essential nutrients to plants, enhancing nutrient uptake and availability, thus supporting vital metabolic processes necessary for growth [66]. Additionally, NPs can optimize light absorption and utilization, improving photosynthetic efficiency. This results in an increased production of energy-rich compounds like sugars, which fuel growth [25]. Moreover, seed priming with NPs can trigger signaling pathways that stimulate cell division and elongation, contributing to overall plant growth [26]and can also reinforce cell membranes, preventing damage and ion leakage. This provides a stable environment for cellular processes that drive growth. Therefore, the utilization of CuO-NPs has been observed to elevate plant growth and photosynthesis while concurrently reducing metal uptake and oxidative stress, as documented in numerous preceding studies. Upon application, CuO-NPs can modulate the enzymatic activities associated with the AsA-GSH cycle, such as ascorbate peroxidase (APX) and glutathione reductase (GR) [67]. This modulation boosts the conversion rates of oxidized ascorbate (DHA) to reduced ascorbate (AsA) and oxidized glutathione (GSSG) to reduced glutathione (GSH), respectively, enhancing the plant's ability to counteract oxidative stress [25, 68]. CuO-NPs, due to their small size and unique surface properties, can interact with cellular membranes, potentially stabilizing them and reducing cellular fractionation [25]. By mitigating membrane disruption, CuO-NPs help maintain cellular compartmentalization, ensuring the optimal functioning of intracellular processes [66]. In addition, CuO-NPs possess a high affinity for metal ions due to their unique physicochemical properties, facilitating adsorption and sequestration of metals at the nano-soil interface, thereby reducing their uptake by plant roots [69]. Additionally, the interaction between CuO-NPs and metal ions can lead to the formation of less bioavailable complexes in the soil, further impeding the translocation of metals into plant tissues [70]. For a comprehensive overview of the combined effects of PVC−MPs and As on *H. vulgare* plants, and the ameliorative influence of CuO−NPs, refer to Fig. 7.

Environmental implication

The presence of PVC−MPs and As in agricultural soils presents significant environmental threats, as both are known to disrupt plant growth, physiology, and overall disturbs ecosystem [18, 30]. Elevated levels of these contaminants can lead to decreased crop yields and may compromise the quality of produce, posing potential risks to food security [12]. The accumulation of PVC−MPs and As in plants could eventually make their way up the food chain, impacting human and animals also [65]. However, the application of CuO−NPs as demonstrated in our study offers a promising strategy to alleviate these detrimental effects of PVC−MPs and As [16, 17]. Additionally, CuO−NPs not only enhance plant resilience against PVC−MPs and As stresses but, crucially, they have the potential to bind to As in the soil, reducing its bioavailability to plants. This mechanism could lead to a decrease in As content in agricultural produce, and also overcome the toxic effects of PVC−MPs, thus safeguarding both ecological balance and human health. The broader application of CuO−NPs in contaminated soils could serve as a sustainable and efficient solution for

restoring soil properties and thus, promoting safer agricultural practices.

Conclusion

In summary, our findings indicate that both PVC−MPs and As stress exert detrimental effects on the growth and ecophysiology of *H. vulgare* plants. Moreover, the escalation of PVC−MPs and As in the soil considerably heightens oxidative stress by increases ROS, disrupts antioxidant activities, and fosters increased proline related parameters, AsA−GSH cycle, and alterations in cellular fractionation. The adverse effects stemming from PVC−MPs and As can be ameliorated through the application of CuO-NPs. This intervention not only diminishes oxidative stress and proline related parameters but also enhances crop yield and productivity. Hence, it is imperative to conduct long-term field studies that establish connections between plant/crop root exudations, metal stress, Cu fertigation strategies, nutrient mobility patterns, and plant growth.

Supplementary Information

The online version contains supplementary material available at https://doi.org/10.1186/s12870-024-05661-w.

Supplementary Material 1

Acknowledgements
The authors extend their appreciation to the Deputyship for Research & Innovation, Ministry of Education in Saudi Arabia for funding this research work through the project number: 223202.

Author contributions
HASA, SMSA, IMA: Conceptualization, Data curation, Writing – original draft, Formal analysis; SAA, DBES, ZKA, SMA, SE: Formal analysis, Validation, Visualization Resources, Writing – review & editing; SJ, SA, TM, BA: Data Curation, Formal analysis, Software, Visualization, Writing – original draft, Writing – review & editing. All authors contributed significantly, have read and agreed to the published version of the manuscript."

Funding
Not applicable.

Data availability
All data generated or analysed during this study are included in this published article.

Declarations

Ethics approval and consent to participate
Barley seeds (*Hordeum vulgare* L.), sourced from the research institute of Hohai University, Nanjing, China. All the experiments were performed in accordance with relevant guidelines and regulations".

Consent for publication
Not applicable.

Competing interests
The authors declare no competing interests.

Author details
[1]Biology Department, College of Science, Jouf University, Sakaka, Aljouf 2014, Saudi Arabia
[2]Department of Biology, College of Science, Qassim University, Burydah 52571, Saudi Arabia
[3]Department of Biology, Faculty of Science, University of Tabuk, Tabuk 71491, Saudi Arabia
[4]Department of Plant Sciences, Quaid-i-Azam University, Islamabad 45320, Pakistan
[5]Department of Biomedical Sciences, Institute of Health, Jimma University, Jimma 378, Ethiopia
[6]Department of Biochemistry, Government College University, Faisalabad 38000, Pakistan
[7]Department of Environmental Sciences and Engineering, Government College University, Faisalabad 38000, Pakistan
[8]Department of Biological Sciences and Technology, China Medical University, Taichung, Taiwan
[9]Department of Horticulture, Agricultural Faculty, Ataturk University, Erzurum 25240, Türkiye
[10]HGF Agro, Ata Teknokent, Erzurum TR-25240, Türkiye
[11]Botany Department, Faculty of Science, Mansoura University, Mansoura 35511, Egypt
[12]Adjunct Faculty, Division of Research and Development, Lovely Professional University, Phagwara 144411, India
[13]School of Science, Western Sydney University, Penrith 2751, Australia

Received: 12 December 2023 / Accepted: 2 October 2024
Published online: 19 October 2024

References

1. Li Y-Q, et al. Effects of polyvinylchloride microplastics on the toxicity of nanoparticles and antibiotics to aerobic granular sludge: Nitrogen removal, microbial community and resistance genes. Environ Res. 2023;238:117151.
2. Xia X, et al. Polyvinyl chloride microplastics induce growth inhibition and oxidative stress in Cyprinus carpio var. Larvae. Sci Total Environ. 2020;716:136479.
3. Yan Y, et al. Effect of polyvinyl chloride microplastics on bacterial community and nutrient status in two agricultural soils. Bull Environ Contam Toxicol. 2021;107:602–9.
4. Ouyang Z, et al. The photo-aging of polyvinyl chloride microplastics under different UV irradiations. Gondwana Res. 2022;108:72–80.
5. Ma J, et al. Effect of microplastic size on the adsorption behavior and mechanism of triclosan on polyvinyl chloride. Environ Pollut. 2019;254:113104.
6. Miao F, et al. Degradation of polyvinyl chloride microplastics via an electro-Fenton-like system with a TiO2/graphite cathode. J Hazard Mater. 2020;399:123023.
7. Fu D, et al. Aged microplastics polyvinyl chloride interact with copper and cause oxidative stress towards microalgae Chlorella vulgaris. Aquat Toxicol. 2019;216:105319.
8. Nosova AO, Uspenskaya MV. Ecotoxicological effects and detection features of polyvinyl chloride microplastics in soils: a review. Environ Adv. 2023;13:100437.
9. Khan MA, et al. Influence of polyvinyl chloride microplastic on chromium uptake and toxicity in sweet potato. Ecotoxicol Environ Saf. 2023;251:114526.
10. Wu H, et al. Toxicity of polyvinyl chloride microplastics on Brassica rapa. Environ Pollut. 2023;336:122435.
11. Al-Huqail AA, Alghanem SMS, Alghamdi SA, Alhaithoul HAS, Al-Robai SA, Alawy AI, et al. Coactive application of Bacillus mycoides PM35 and calcium oxide nanoparticles stimulate eco-physiological responses in maize (*Zea mays* L.) under chromium stress. J Soil Sci Plant Nutr. 2024.
12. Ma J, et al. Interaction of titanium dioxide nanoparticles with PVC-microplastics and chromium counteracts oxidative injuries in Trachyspermum ammi L. by modulating antioxidants and gene expression. Ecotoxicol Environ Saf. 2024;274:116181.
13. Alhaithloul HAS, Ali B, Alghanem SMS, Zulfiqar F, Al-Robai SA, Ercisli S, et al. Effect of green-synthesized copper oxide nanoparticles on growth, physiology, nutrient uptake, and cadmium accumulation in Triticum aestivum (L.). Ecotoxicol Environ Saf. 2023;268:115701.
14. Alwutayd KM, Alghanem SMS, Alwutayd R, Alghamdi SA, Alabdallah NM, Al-Qthanin RN, et al. Mitigating chromium toxicity in rice (*Oryza sativa* L.) via

ABA and 6-BAP: Unveiling synergistic benefits on morphophysiological traits and ASA-GSH cycle. Sci Total Environ. 2023;908:168208.
15. Alatawi A, et al. Application of silicon and sodium hydrosulfide alleviates arsenic toxicity by regulating the physio-biochemical and molecular mechanisms of Zea mays. Environmental Science and Pollution Research; 2023.
16. Sun H, et al. Effects of polyethylene and biodegradable microplastics on photosynthesis, antioxidant defense systems, and arsenic accumulation in maize (Zea mays L.) seedlings grown in arsenic-contaminated soils. Sci Total Environ. 2023;868:161557.
17. Alwutayd KM et al. Advancing Arsenic Toxicity Mitigation in Rice (Oryza sativa L.) with Rice Straw Biochar and Silicon: a study on Morpho-Physio-biochemical responses. J Soil Sci Plant Nutr, 2024: pp. 1–15.
18. Ullah I, et al. Phytoremediation of Arsenic (as) in rice plants, mediated by Bacillus subtilis strain IU31 through antioxidant responses and phytohormones synthesis. Environ Pollut. 2024;355:124207.
19. Abeed AHA, Saleem MH, Asghar MA, Mumtaz S, Ameer A, Ali B, et al. Ameliorative effects of exogenous potassium nitrate on antioxidant defence system and mineral nutrient uptake in radish (*Raphanus sativus* L.) under salinity stress. ACS Omega. 2023;8(25):22575–22588.
20. Banerjee S, et al. Rhizospheric nano-remediation salvages arsenic genotoxicity: zinc-oxide nanoparticles articulate better oxidative stress management, reduce arsenic uptake, and increase yield in Pisum sativum (L). Sci Total Environ. 2024;913:169493.
21. Sun Y, et al. New insights in to the ameliorative effects of zinc and iron oxide nanoparticles to arsenic stressed spinach (Spinacia oleracea L). Plant Physiol Biochem. 2023;107715:p.
22. Irshad MA, Sattar S, Al-Huqail AA, Alghanem SM, Nawaz R, Ain NU, et al. Green synthesis and characterization of silver and copper nanoparticles and their use as an effective adsorbent for chromium removal and recovery from wastewater. Environ Sci Pollut Res. 2023;30(52):112575–112590.
23. Patowary R, Devi A, Mukherjee AK. Advanced bioremediation by an amalgamation of nanotechnology and modern artificial intelligence for efficient restoration of crude petroleum oil-contaminated sites: a prospective study. Environmental Science and Pollution Research; 2023. pp. 1–26.
24. Kim D-Y et al. Bioinspired silver nanoparticle-based nanocomposites for effective control of plant pathogens: a review. Sci Total Environ, 2023: p. 168318.
25. Peng C, et al. Proteomic analysis unravels response and antioxidation defense mechanism of rice plants to copper oxide nanoparticles: comparison with bulk particles and dissolved Cu ions. Volume 2. ACS Agricultural Science & Technology; 2022. pp. 671–83. 3.
26. Shah IH, et al. Green synthesis and characterization of copper oxide nanoparticles using Calotropis procera leaf extract and their different biological potentials. J Mol Struct. 2022;1259:132696.
27. Hassan A, et al. Foliar application of ascorbic acid enhances salinity stress tolerance in barley (Hordeum vulgare L.) through modulation of morpho-physio-biochemical attributes, ions uptake, osmo-protectants and stress response genes expression. Saudi Journal of Biological Sciences; 2021.
28. Hassan A et al. Oxidative stress alleviation as indicated by enzymatic and nonenzymatic antioxidants and osmoregulators in barley (Hordeum vulgare l.) under salt (NaCl) stress by ascorbic acid (ASA). Pak J Bot, 2020. 54(1).
29. Ma J et al. Short-term responses of spinach (Spinacia oleracea L.) to the individual and combinatorial effects of Nitrogen, Phosphorus and Potassium and silicon in the soil contaminated by boron. Front Plant Sci, 2022. 13.
30. Al-Huqail AA, et al. Combined exposure of PVC-microplastic and mercury chloride (HgCl2) in sorghum (Pennisetum glaucum L.) when its seeds are primed titanium dioxide nanoparticles (TiO2–NPs). Environmental Science and Pollution Research; 2024.
31. Manzoor N, et al. Comparative efficacy of silicon and iron oxide nanoparticles towards improving the plant growth and mitigating arsenic toxicity in wheat (Triticum aestivum L). Ecotoxicol Environ Saf. 2023;264:115382.
32. Wang Y, et al. Phytotoxicity of microplastics to the floating plant Spirodela polyrhiza (L.): plant functional traits and metabolomics. Environ Pollut. 2023;322:121199.
33. Saleem MH, et al. Silicon enhances Morpho–physio–biochemical responses in Arsenic stressed spinach (Spinacia oleracea L.) by minimizing its Uptake. Journal of Plant Growth Regulation; 2022.
34. Ge J, et al. Review of the toxic effect of microplastics on terrestrial and aquatic plants. Sci Total Environ. 2021;791:148333.
35. Javed MT, et al. Changes in pH and organic acids in mucilage of Eriophorum angustifolium roots after exposure to elevated concentrations of toxic elements. Environ Sci Pollut Res. 2013;20(3):1876–80.
36. Greger M, Landberg T. Role of rhizosphere mechanisms in cd uptake by various wheat cultivars. Plant Soil. 2008;312(1):195–205.
37. Arnon DI. Copper enzymes in isolated chloroplasts. Polyphenoloxidase in Beta vulgaris. Plant Physiol. 1949;24(1):1.
38. Austin RB. *Prospects for genetically increasing the photosynthetic capacity of crops*. 1990.
39. Heath RL, Packer L. Photoperoxidation in isolated chloroplasts: I. kinetics and stoichiometry of fatty acid peroxidation. Arch Biochem Biophys. 1968;125(1):189–98.
40. Jana S, Choudhuri MA. Glycolate metabolism of three submersed aquatic angiosperms: effect of heavy metals. Aquat Bot. 1981;11:67–77.
41. Dionisio-Sese ML, Tobita S. Antioxidant responses of rice seedlings to salinity stress. Plant Sci. 1998;135(1):1–9.
42. Chen C-N, Pan S-M. Assay of superoxide dismutase activity by combining electrophoresis and densitometry. Botanical Bulletin of Academia Sinica; 1996. p. 37.
43. Sakharov IY, Ardila GB. Variations of peroxidase activity in cocoa (Theobroma cacao L.) beans during their ripening, fermentation and drying. Food Chem. 1999;65(1):51–4.
44. Aebi H. *[13] catalase in vitro*, in *methods in enzymology*. Elsevier; 1984. pp. 121–6.
45. Nakano Y, Asada K. Hydrogen peroxide is scavenged by ascorbate-specific peroxidase in spinach chloroplasts. Plant Cell Physiol. 1981;22(5):867–80.
46. El-Esawi MA, et al. Serratia marcescens BM1 enhances cadmium stress tolerance and phytoremediation potential of soybean through modulation of osmolytes, leaf gas exchange, antioxidant machinery, and stress-responsive genes expression. Antioxidants. 2020;9(1):43.
47. Sirhindi G, et al. Jasmonic acid modulates the physio-biochemical attributes, antioxidant enzyme activity, and gene expression in Glycine max under nickel toxicity. Front Plant Sci. 2016;7:591.
48. Pękal A, Pyrzynska K. Evaluation of aluminium complexation reaction for flavonoid content assay. Food Anal Methods. 2014;7(9):1776–82.
49. Bray H, Thorpe W. *Analysis of phenolic compounds of interest in metabolism*. Methods of biochemical analysis, 1954: pp. 27–52.
50. Lewis CE, et al. Determination of anthocyanins, flavonoids and phenolic acids in potatoes. I: coloured cultivars of Solanum tuberosum L. J Sci Food Agric. 1998;77(1):45–57.
51. Dubois M, et al. Colorimetric method for determination of sugars and related substances. Anal Chem. 1956;28(3):350–6.
52. Bates LS, Waldren RP, Teare I. Rapid determination of free proline for water-stress studies. Plant Soil. 1973;39(1):205–7.
53. Singh MK, et al. Response of different doses of NPK and Boron on Growth and Yield of Broccoli (Brassicaoleracea L. var. Italica). Int J Bio-resource Stress Manage. 2015;6(1):108–12.
54. Yang Q-w, et al. Concentration and potential health risk of heavy metals in market vegetables in Chongqing, China. Ecotoxicol Environ Saf. 2011;74(6):1664–9.
55. Liu Y-Q, et al. Plant growth-promoting bacteria modulate gene expression and induce antioxidant tolerance to alleviate synergistic toxicity from combined microplastic and cd pollution in sorghum. Ecotoxicol Environ Saf. 2023;264:115439.
56. Zhuang H, et al. Combination of transcriptomics, metabolomics and physiological traits reveals the effects of polystyrene microplastics on photosynthesis, carbon and nitrogen metabolism in cucumber (Cucumis sativus L). Plant Physiol Biochem. 2023;205:108201.
57. Ma J, et al. Effects of microplastics on growth and metabolism of rice (Oryza sativa L). Chemosphere. 2022;307:135749.
58. Amin F, AL-Huqail AA, Ullah S, Khan MN, Kaplan A, Ali B*, et al. Mitigation effect of alpha-tocopherol and thermo-priming in *Brassica napus* L. under induced mercuric chloride stress. BMC Plant Biol. 2024;24(1):108.
59. Pignattelli S, Broccoli A, Renzi M. Physiological responses of garden cress (L. Sativum) to different types of microplastics. Sci Total Environ. 2020;727:138609.
60. Kaya C et al. *Silicon is dependent on hydrogen sulphide to improve boron toxicity tolerance in pepper plants by regulating the AsA-GSH cycle and glyoxalase system*. Chemosphere, 2020: p. 127241.
61. Ozfidan-Konakci C, et al. Hydrogen sulfide (H2S) and nitric oxide (NO) alleviate cobalt toxicity in wheat (Triticum aestivum L.) by modulating photosynthesis, chloroplastic redox and antioxidant capacity. J Hazard Mater. 2020;388:122061.

62. Sun Y, et al. Combined application of plant growth-promoting bacteria and iron oxide nanoparticles ameliorates the toxic effects of arsenic in Ajwain (Trachyspermum ammi L). Front Plant Sci. 2022;13:1098755.
63. Gupta P, Seth CS. Nitrate supplementation attenuates as (V) toxicity in Solanum lycopersicum L. Cv Pusa Rohini: insights into as (V) sub-cellular distribution, photosynthesis, nitrogen assimilation, and DNA damage. Plant Physiol Biochem. 2019;139:44–55.
64. Irshad S, et al. Biochar composite with microbes enhanced arsenic biosorption and phytoextraction by Typha latifolia in hybrid vertical subsurface flow constructed wetland. Environ Pollut. 2021;291:118269.
65. Alshegaihi RM, Mfarrej MFB, Saleem MH, Parveen A, Ahmad KS, Ali B, et al. Effective citric acid and EDTA treatments in cadmium stress tolerance in pepper (*Capsicum annuum* L.) seedlings by regulating specific gene expression. South Afr J Botany 2023;159:367–380.
66. Saleem MH, et al. Synthesis, characterization, and advanced sustainable applications of copper oxide nanoparticles: a review. Clean Technologies and Environmental Policy; 2024. pp. 1–26.
67. Waris A, et al. A comprehensive review of green synthesis of copper oxide nanoparticles and their diverse biomedical applications. Inorg Chem Commun. 2021;123:108369.
68. Mo F, et al. Biological effects of silver ions to Trifolium pratense L. revealed by analysis of biochemical indexes, morphological alteration and genetic damage possibility with special reference to hormesis. Environ Exp Bot. 2021;186:104458.
69. Tortella G, et al. Silver, copper and copper oxide nanoparticles in the fight against human viruses: progress and perspectives. Crit Rev Biotechnol. 2022;42(3):431–49.
70. Alshegaihi RM, et al. Silicon and Titanium Dioxide mitigate copper stress in wheat (Triticum aestivum L.) through regulating antioxidant defense mechanisms. Journal of Plant Growth Regulation; 2023.

Publisher's note